SCIENTIFIC REPORTS
nature research

OPEN

In vitro study of interaction of 17β-hydroxysteroid dehydrogenase type 10 and cyclophilin D and its potential implications for Alzheimer's disease

Erika Hemmerová[1], Tomáš Špringer[1], Zdenka Krištofiková[2] & Jiří Homola[1*]

In early stages of Alzheimer's disease (AD), amyloid-β (Aβ) accumulates in neuronal mitochondria where it interacts with a number of biomolecules including 17beta-hydroxysteroide dehydrogenase 10 (17β-HSD10) and cyclophilin D (cypD). It has been hypothesized that 17β-HSD10 interacts with cypD preventing it from opening mitochondrial permeability transition pores and that its regulation during AD may be affected by the accumulation of Aβ. In this work, we demonstrate for the first time that 17β-HSD10 and cypD form a stable complex *in vitro*. Furthermore, we show that factors, such as pH, ionic environment and the presence of Aβ, affect the ability of 17β-HSD10 to bind cypD. We demonstrate that K^+ and Mg^{2+} ions present at low levels may facilitate this binding. We also show that different fragments of Aβ ($Aβ_{1–40}$ and $Aβ_{1–42}$) affect the interaction between 17β-HSD10 and cypD differently and that $Aβ_{1–42}$ (in contrast to $Aβ_{1–40}$) is capable of simultaneously binding both 17β-HSD10 and cypD in a tri-complex.

Research into interactions between biomolecules represents an important route to the understanding of life at a molecular and cellular level. Expanding the knowledge of molecular processes associated with an onset and progression of a disease is a major challenge for modern science with potential significant implications for the development of new diagnostic and treatment modalities. Surface plasmon resonance (SPR) biosensors are an essential technology for the real-time label-free investigation of biomolecular interactions[1]. In recent years, SPR biosensors have been applied for the study of interactions of a variety of biomolecules (e.g., proteins, nucleic acids, and lipids), providing new insights into equilibrium and kinetic aspects of biomolecular interactions and relationships between interacting biomolecules (e.g., binding stoichiometry, epitope mapping)[2,3]. In this work, we use SPR biosensor technology to investigate interactions of proteins implicated in Alzheimer's disease (AD).

AD is a chronic neurodegenerative disease that is characterized by the progressive decline of memory and cognitive functions due to extensive neuronal death, and despite decades of intensive research, the progression of the disease is still not fully understood and therefore no effective cure is yet available. One of the main pathological hallmarks found in the affected parts of brains of AD patients are senile plaques formed by the aggregates of extracellular amyloid-β peptide (Aβ). Aβ is a peptide released at different sizes, of which 40aa long residues ($Aβ_{1–40}$) represent ~80–90% of the physiologically secreted Aβ fragments, followed by 42aa long residues ($Aβ_{1–42}$) representing ~5–10% of total Aβ fragments[4]. During AD, mutations in the cleavage pathway can lead to an increased production of Aβ and/or preferential production of $Aβ_{1–42}$ over $Aβ_{1–40}$ leading to oligomerization of Aβ and formation of aggregates[5–7]. As $Aβ_{1–42}$ is more prone to the oligomerization than $Aβ_{1–40}$[8,9], it plays a crucial pathological role in AD. Recent studies suggest that the role of Aβ in AD may be more complex than just the formation of plaques[10,11]. It has been highlighted that in early stages of AD, Aβ enters neuronal cells and accumulates, among other places, in the synaptic mitochondria[12,13]. Inside mitochondria, it binds other biomolecules of mitochondrial matrix, such as 17beta−hydroxysteroid dehydrogenase type 10 (17β-HSD10)[14–16] or cyclophilin D (cypD)[17,18] and thereby contributes to the progression of AD.

[1]Institute of Photonics and Electronics of the Czech Academy of Sciences, Chaberská 57, 182 51, Prague, Czech Republic. [2]National Institute of Mental Health, Topolová 748, 250 67, Klecany, Czech Republic. *email: homola@ufe.cz

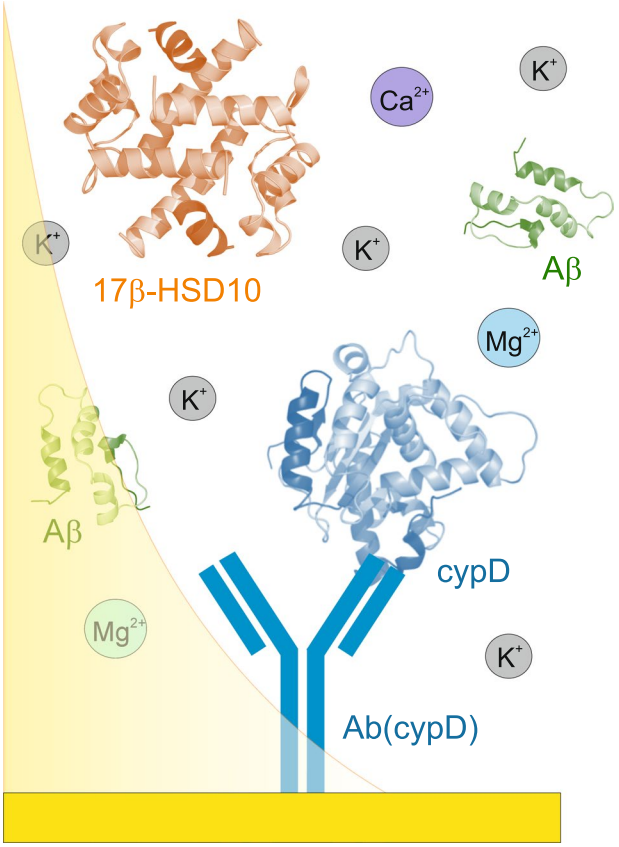

Figure 1. Design of the experimental layout for investigation of the interaction between 17β-HSD10 and cypD using an SPR biosensor.

17β-HSD10 is a protein which is involved in mitochondrial metabolism[19] and in the maintenance of mitochondrial integrity under metabolic stress[20]. The interaction between 17β-HSD10 and monomeric Aβ has very little effect on the enzymatic function of 17β-HSD10[14]; however, the oligomeric Aβ inhibits its activity as it changes the conformation of 17β-HSD10 preventing it from binding its cofactor NAD^+[21]. CypD is also located in the mitochondrial matrix and due to oxidative and other cellular stresses may be translocated to the inner mitochondrial membrane. This leads to the formation and opening of mitochondrial permeability transition pores (mPTP), resulting in the collapse of membrane potential and activation of apoptotic cell mechanisms[18,22]. Both fragments of Aβ ($Aβ_{1–40}$ and $Aβ_{1–42}$) interact with cypD; $Aβ_{1–42}$ exhibiting higher affinity to cypD than $Aβ_{1–40}$ and the oligomeric form exhibiting higher affinity to cypD than the monomeric form[17,18].

Interactions of Aβ with both 17β-HSD10 and cypD were linked with pathological processes, such as disturbed mitochondrial energy metabolism, Ca^{2+} homeostasis, membrane potential change, generation of reactive oxygen species (ROS) and other mitochondrial dysfunctions[23,24]. In addition, it was hypothesized that 17β-HSD10 and cypD form a complex and that excessive accumulation of Aβ during AD may disrupt this complex resulting in the upregulation of free cypD, increased mPTP opening and pronounced apoptosis. However, this hypothesis was based on studies using indirect methods, such as fluorescence co-localization or immunoprecipitation[14,25], and no direct proof of the binding between 17β-HSD10 and cypD has been provided yet.

In this work, we use the SPR biosensor method to study the interaction between 17β-HSD10 and cypD in a direct manner and under variable physiologically relevant environmental conditions (Fig. 1). As the concentration of ions in the mitochondrial matrix fluctuates in response to the perturbations in the cytosolic environment as well as to the temporal metabolic processes[26,27], we study the effect of ions on this interaction. In particular, we investigate how the binding between 17β-HSD10 and cypD is influenced by concentrations of the most relevant ions, such as K^+, Mg^{2+}, and Ca^{2+}. Finally, in order to explore the hypothesis proposed by Yan and Stern, we evaluate the effect of the presence of two different Aβ fragments, $Aβ_{1–40}$ and $Aβ_{1–42}$ (exhibiting different oligomerization dispositions) on the interaction between 17β-HSD10 and cypD to enable deeper understanding of processes taking places during the early stages of AD.

Results

Study of interaction between 17β-HSD10 and cypD under variable environmental conditions. In this part, we present the results of our study of the interaction between 17β-HSD10 and cypD under different environmental conditions, such as pH and concentrations of ions. As physiological values of pH in the mitochondrial matrix are believed to be 7.8[28] or lower (down to 7.0)[29], we considered two pH values - 7.4 and 7.8. The concentration range for K^+ and Mg^{2+} (the most abundant mono- and bi-valent ions present in

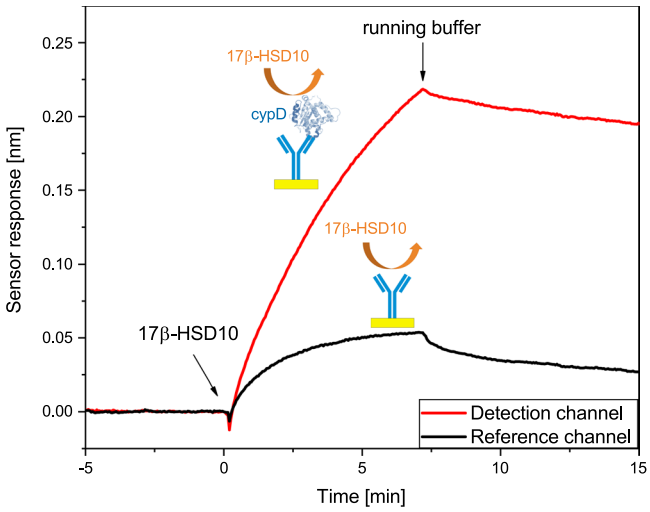

Figure 2. Sensorgram corresponding to the binding of 17β-HSD10 to the surface with and without immobilized cypD.

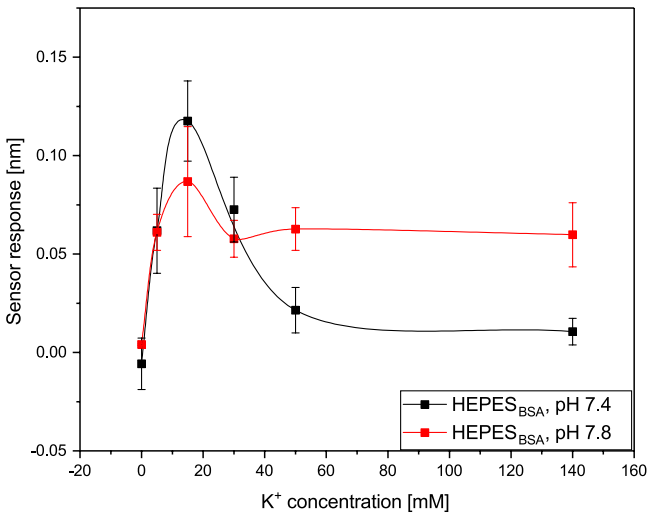

Figure 3. Dependence of the binding between 17β-HSD10 and cypD on concentration of K^+ obtained at a pH of 7.4 and 7.8.

the mitochondrial matrix) was selected to span from 0 mM to the physiological concentrations reported for the mitochondrial matrix: 140 mM for K^+[30] and 2.5 mM for Mg^{2+}[31]. While the binding experiments were performed at a temperature of 25 °C for all the selected combinations of environmental parameters to facilitate comparison with the previous studies, the selected experiments were repeated at a physiologically more relevant temperature of 37 °C to assess the effect of temperature.

Figure 2 shows the sensorgram corresponding to the binding of 17β-HSD10 to the surface of the sensor with and without immobilized cypD. A much higher sensor response can be seen in the sensor channel with immobilized cypD, which indicates that 17β-HSD10 recognizes cypD and is able to bind to it. After the supply of 17β-HSD10 is interrupted (t = 7 minutes), the sensor response in the sensor channel with the immobilized cypD decreases only slightly which implies that the complex formed by 17β-HSD10 and cypD is stable.

Figures 3 and 4 show the dependence of the sensor response (corresponding to the binding of 17β-HSD10 to the immobilized cypD) on the concentration of K^+ and Mg^{2+} measured at two different pH values. For all the types of ions and pH values, the data indicate that the efficiency of the binding between 17β-HSD10 and cypD approaches zero in the absence of ions and increases with an increasing concentration of ions, until it reaches a maximum value. A further increase in the concentration of ions results in a decrease in the binding efficiency. However, whereas the concentration of K^+ corresponding to the maximum binding efficiency is about the same (15 mM) for both pH values, the maximum binding efficiency in the presence of Mg^{2+} ions occurs at 1 μM (pH 7.8) and 0.25 mM (pH 7.4). In addition, the binding is more pronounced in the presence of Mg^{2+} than in the presence of K^+ (for both the pH values, albeit only slightly at pH 7.8) and at a pH of 7.4 than at a pH of 7.8 (for both types of ions). Therefore, a pH of 7.4 was selected for use in further studies.

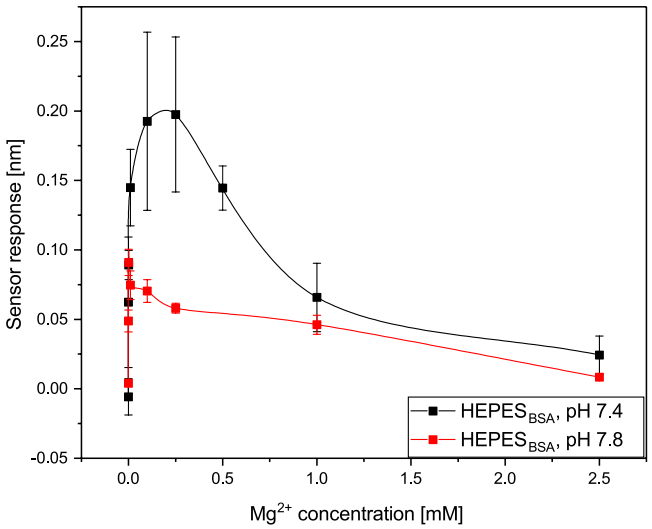

Figure 4. Dependence of the binding between 17β-HSD10 and cypD on concentration of Mg^{2+} obtained at a pH of 7.4 and 7.8.

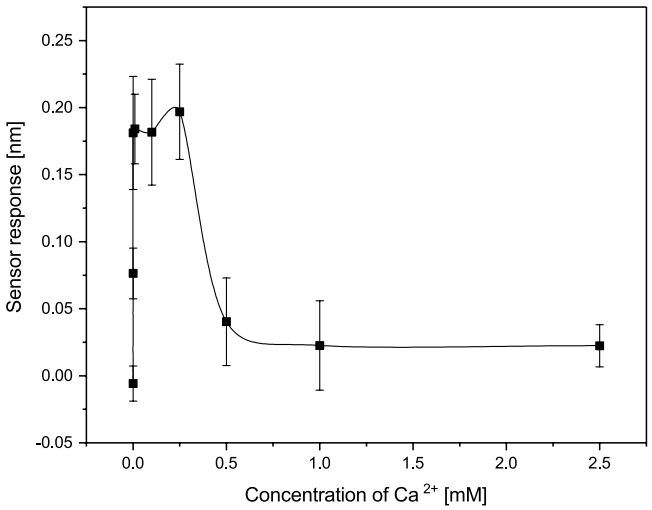

Figure 5. Dependence of the binding between 17β-HSD10 and cypD on concentration of Ca^{2+} obtained at a pH of 7.4.

In order to further characterize the effect of ions on the interaction between 17β-HSD10 and cypD, we studied the effect of Ca^{2+} ions that play a prominent role in mitochondrial metabolism[32] and apoptosis[33]. As follows from Fig. 5, the binding efficiency between 17β-HSD10 and cypD in the presence of Ca^{2+} follows the same trend as the binding efficiency in the presence of the other two ions and the maximum binding efficiency takes place at a concentration of Ca^{2+} of 0.25 mM.

The mixture of ions inside the mitochondrial matrix may collectively affect biomolecular interactions in mitochondria. Therefore, besides the investigation of the effect of individual ions on the binding between 17β-HSD10 and cypD, we also studied the effect of simultaneously present K^+ and Mg^{2+} ions. In this study, we kept the concentration of one ion constant (at the concentration for which the binding efficiency was the highest) and varied the concentration of the other. The corresponding results in Figs 6 and 7 illustrate how the presence of K^+ and Mg^{2+} influences the binding between 17β-HSD10 and cypD.

The results depicted in Fig. 6 indicate that at low Mg^{2+} concentrations, the presence of 15 mM K^+ increases the binding efficiency, whereas at higher Mg^{2+} concentrations, the binding efficiency in the presence of both K^+ and Mg^{2+} is comparable with that measured in the presence of Mg^{2+} only. Furthermore, Fig. 7 suggests that at low K^+ concentrations, the presence of 0.25 mM Mg^{2+} increased the efficiency of binding between 17β-HSD10 and cypD. A further increase in K^+ concentration resulted in a decrease in the binding efficiency for both the combined K^+ and Mg^{2+} and individual K^+. The binding efficiency was approximately twice as high for combined Mg^{2+} and K^+ in comparison with that measured in the presence of K^+ only.

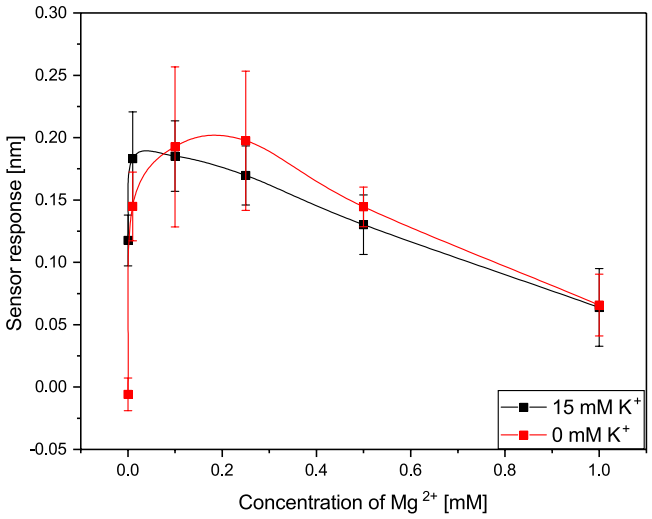

Figure 6. Dependence of the binding of 17β-HSD10 to cypD on concentration of Mg^{2+} in the presence and absence of 15 mM K^{+} obtained at a pH of 7.4.

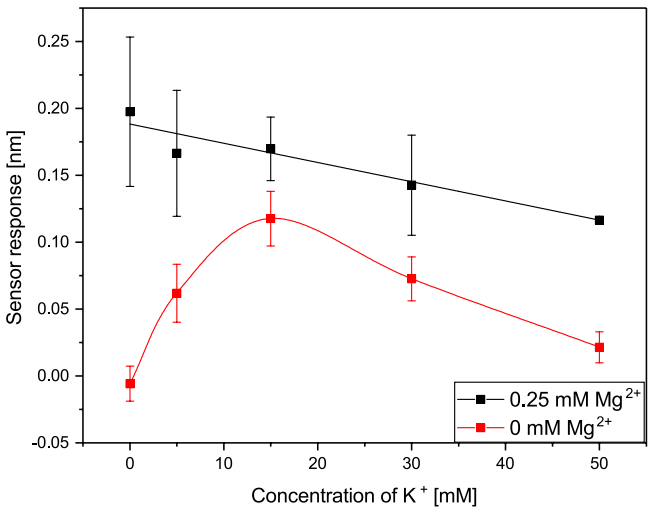

Figure 7. Dependence of the binding of 17β-HSD10 to cypD on concentration of K^{+} in the presence and absence of 0.25 mM Mg^{2+} obtained at a pH of 7.4.

Based on these experiments, HEPES with 15 mM K^{+} and 0.1 mM Mg^{2+} was selected to be used in further experiments as these conditions appear to favour binding between 17β-HSD10 and cypD.

As follows from Supplementary Fig. S2 and Supplementary Table S3 (see Supplementary Information), 17β-HSD10 and cypD form a complex both at 37 °C and 25 °C. In addition, the interactions of 17β-HSD10 and cypD realized at the two different temperatures generated only slightly different sensor responses (within the error of the measurement).

Study of interaction between 17β-HSD10 and cypD in the presence of Aβ. We evaluated whether and how the presence of $A\beta_{1-40}$ or $A\beta_{1-42}$ influences the interaction between 17β-HSD10 and cypD. Figure 8 shows sensorgrams corresponding to the binding of 17β-HSD10 incubated with Aβ ($A\beta_{1-40}$ or $A\beta_{1-42}$), and the binding of individual 17β-HSD10, $A\beta_{1-40}$ and $A\beta_{1-42}$ to cypD immobilized on the surface of an SPR chip. There is a substantial difference in the effect of the two different types of Aβ. $A\beta_{1-40}$ incubated with 17β-HSD10 generates a sensor response that is lower than individual 17β-HSD10 and comparable to that of individual $A\beta_{1-40}$. In contrast, $A\beta_{1-42}$ incubated with 17β-HSD10 generates a sensor response that is higher than the sensor responses corresponding to the individual binding partners (17β-HSD10 or $A\beta_{1-42}$), and is even higher than the two added together.

The results of the interaction study obtained with one of the interacting partners (cypD) immobilized on the surface of an SPR sensor were compared to those obtained with all interacting partners present in solution. In this experimental format, cypD, 17β-HSD10 and Aβ ($A\beta_{1-40}$ or $A\beta_{1-42}$) were incubated in solution and flowed along Ab(cypD) that was immobilized on the surface of an SPR chip. Subsequently, the chip was

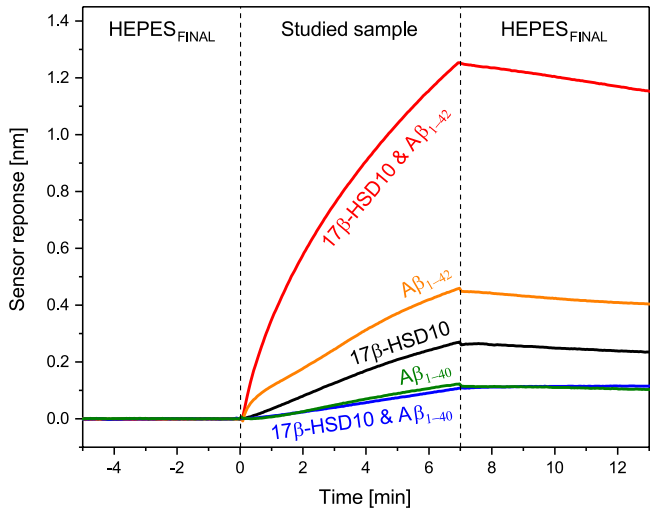

Figure 8. Sensorgram corresponding to the binding of 17β-HSD10 incubated with Aβ (Aβ$_{1-40}$ or Aβ$_{1-42}$), and the binding of individual 17β-HSD10, Aβ$_{1-42}$ and Aβ$_{1-40}$ to the immobilized cypD.

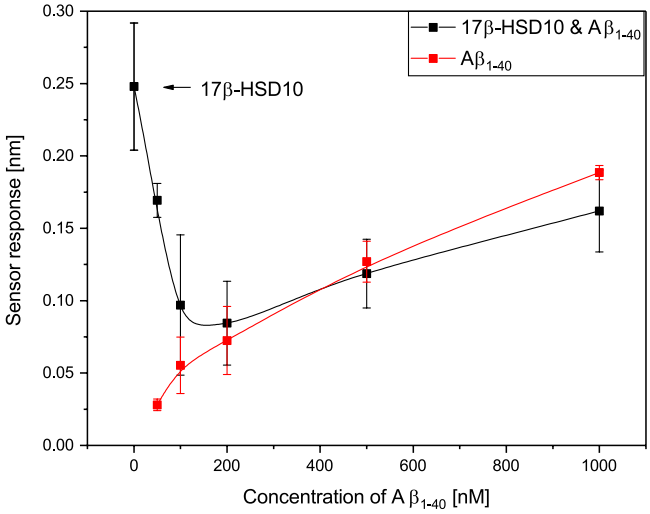

Figure 9. Dependence of the binding of Aβ$_{1-40}$ and Aβ$_{1-40}$ incubated with17β-HSD10 to the immobilized cypD on concentration of Ab$_{1-40}$.

exposed to Ab(17β-HSD10) to confirm the capture of 17β-HSD10. Supplementary Fig. S3 (see Supplementary Information) shows the binding of Ab(17β-HSD10) to the sensor surface that was previously exposed to the mixture of 17β-HSD10 and cypD, which confirms that the 17β-HSD10/cypD complex was formed. 17β-HSD10 and cypD incubated with Aβ$_{1-42}$ generates a sensor response to Ab(17β-HSD10) that is about 6 times higher than 17β-HSD10 and cypD incubated in the absence of Aβ$_{1-42}$; the incubation with Aβ$_{1-40}$ reduces the sensor response to Ab(17β-HSD10) by about one half. The binding of Ab(17β-HSD10) to the sensor surface exposed to reference solutions containing different combinations of the interacting molecules (Solutions 4–12 in Supplementary Table S2) produces sensor responses significantly smaller than those obtained when using solutions of cypD, 17β-HSD10 and Aβ (see Supplementary Fig. S4). This confirms that the binding was specific.

The data collected in both experimental formats indicates that: 1) Aβ$_{1-40}$ as well as Aβ$_{1-42}$ bind both 17β-HSD10 and cypD and 2) Aβ$_{1-42}$ forms a complex with 17β-HSD10 and cypD containing all three binding partners (a tri-complex), whereas Aβ$_{1-40}$ is not able to interact simultaneously with both proteins. This implies that the binding of free Aβ$_{1-40}$ that is present in the sample in excess, would be responsible for the majority of the sensor response to the binding of the mixture of 17β-HSD10 with Aβ$_{1-40}$ shown in Fig. 8.

In order to confirm this hypothesis and to correlate the sensor response generated by the binding of Aβ$_{1-40}$ incubated with 17β-HSD10 to the excess of Aβ$_{1-40}$ in the mixture, the sensor response to mixtures with different concentrations of Aβ$_{1-40}$ was measured (molar ratio of Aβ$_{1-40}$ to 17β-HSD10 ranging from 1:2 to 10:1, with the concentration of 17β-HSD10 kept constant). As depicted in Fig. 9, the sensor response to individual Aβ$_{1-40}$ increased with an increasing concentration of Aβ$_{1-40}$. Conversely, the sensor response to Aβ$_{1-40}$ incubated with 17β-HSD10 decreased with an increasing concentration of Aβ$_{1-40}$ until it became comparable with the sensor

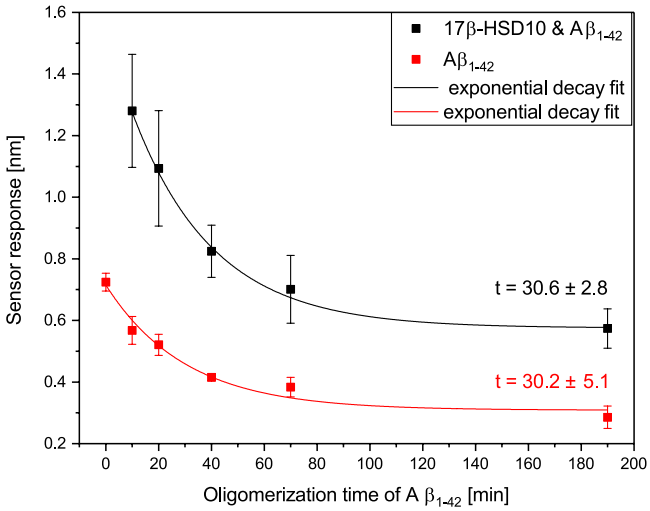

Figure 10. Dependence of the binding of $A\beta_{1-42}$ and 17β-HSD10/$A\beta_{1-42}$ to the immobilized cypD on oligomerization time of $A\beta_{1-42}$.

response corresponding to the binding of individual $A\beta_{1-40}$ (around a concentration of $A\beta_{1-40}$ of 200 nM) and then it started to grow following the same trend as that observed for the binding of individual $A\beta_{1-40}$. This suggests that $A\beta_{1-40}$ binds 17β-HSD10 and the formed complex is not able to bind to cypD. Therefore, at low concentrations of $A\beta_{1-40}$, the sensor response is predominantly caused by the binding of 17β-HSD10, whereas at high concentrations of $A\beta_{1-40}$, it is caused mainly by the binding of free $A\beta_{1-40}$. Results of analogous experiments performed with a variable concentration of $A\beta_{1-42}$ are shown in Supplementary Fig. S5 (see Supplementary Information). Figure S5 shows that the sensor response to the binding of $A\beta_{1-42}$ to cypD immobilized on the sensor surface increases linearly with an increasing concentration $A\beta_{1-42}$. The sensor response to the binding of $A\beta_{1-42}$ incubated with 17β-HSD10 to the immobilized cypD exhibits a more complex behavior: while the sensor response is increasing with the concentration of $A\beta_{1-42}$ in general, there is a pronounced local maximum at a concentration of ~100 nM. While our experiments strongly support this deviation from a monotonous trend of the sensor response (it was confirmed by five independent experiments), we do not have plausible explanation of the mechanisms behind this effect. However, within the considered range of concentrations of $A\beta_{1-42}$, the sensor response to the binding of $A\beta_{1-42}$ incubated with 17β-HSD10 was consistently higher than that corresponding to individual $A\beta_{1-42}$, which confirms the formation of a tri-complex.

In order to better understand the mechanism through which Aβ affects the interaction between 17β-HSD10 and cypD, we studied the effect of the degree of oligomerization of Aβ. In this experiment, Aβ in solution was allowed to form oligomers for different periods of time ("oligomerization time"), and then 17β-HSD10 was added into the mixture and the mixture was injected in the SPR sensor. As follows from Fig. 10, $A\beta_{1-42}$ incubated with 17β-HSD10 generates a sensor response about twice as high as individual $A\beta_{1-42}$. This suggests that the 17β-HSD10/$A\beta_{1-42}$ complex binds to the immobilized cypD, which is in agreement with the data presented in Fig. 8. With increasing $A\beta_{1-42}$ oligomerization time, the binding efficiency of both $A\beta_{1-42}$ as well as 17β-HSD10/$A\beta_{1-42}$ to the immobilized cypD decreases. The fitting of the obtained data with the use of a simple exponential decay function yielded time decay constants of about 30 minutes for both the 17β-HSD10/$A\beta_{1-42}$ complex and individual $A\beta_{1-42}$. For comparison, we carried the same experiments with $A\beta_{1-40}$ and did not observe any dependence of the sensor response on the $A\beta_{1-40}$ oligomerization time. This indicates that its oligomerization requires a considerably longer time under the conditions used, which is consistent with the published data[9,34].

Discussion

In the first part of our study, we have demonstrated that the two mitochondrial proteins, 17β-HSD10 and cypD, interact with each other forming a stable complex. This is the first report that provides evidence of this interaction and supports the hypothesis of Yan and Stern[14]. Furthermore, we have shown (Figs 3–7) that the interaction between 17β-HSD10 and cypD is significantly affected by environmental conditions such as the pH and concentrations of K^+, Mg^{2+} or Ca^{2+}. We observed considerably higher binding efficiencies for K^+, Mg^{2+} or Ca^{2+} present at concentrations within a relatively narrow range and at a lower pH value. Furthermore, our data indicate that the effect of bivalent Ca^{2+} and Mg^{2+} ions was rather similar and much stronger than that of monovalent K^+. This implies that the interaction is not only sensitive to the ionic strength of the environment, but also (at least partially) to the valence of the present ions.

We observed the highest efficiency of the binding between 17β-HSD10 and cypD for a pH of 7.4, and at a concentration of ions around 15 mM of K^+ and 0.1 mM of Mg^{2+}. These values are somewhat lower than the prevalent physiological values in the mitochondrial matrix reported in the literature. However, it should be noted that the mitochondrion is a complex organelle in which concentrations of ions fluctuate in response to metabolic processes and perturbations of the cytosolic environment[26,27]. The data reported in the literature may also be affected by the methodology used. For example, a commonly assumed pH value in mitochondria of 7.8[26,28,30] originates

mostly from studies in which mitochondria were maintained in non-physiological buffers[29]. When mitochondria were maintained under more realistic physiological conditions, considerably lower pH values were observed (down to 7.0[29]). K^+ is commonly assumed to occur in the mitochondria at concentrations around 140 mM[30,35]; however, much lower K^+ concentrations (down to 15 mM) have also been observed[36,37]. Mg^{2+} concentrations in the mitochondrial matrix were determined to fall between 0.5 mM and 2.5 mM[38,39]. Therefore, the conditions under which we observed the most efficient binding of 17β-HSD10 to cypD, may be considered physiological. This suggests that our findings may be applicable to interactions in mitochondria and that indeed 17β-HSD10 is able to regulate cypD in mitochondrial matrix. Subsequently, changes in the ionic balance in mitochondrial matrix may disrupt 17β-HSD10/cypD binding and cause the release of cypD, which may result in the opening of mPTP and trigger apoptotic processes. This is a particularly relevant finding, as an excessive accumulation of Ca^{2+} is known to affect membrane potential through the formation and opening of mPTP[33]. We hypothesize that the process of disruption of membrane potential at high Ca^{2+} concentrations is caused by the Ca^{2+}-induced disruption of the 17β-HSD10/cypD complex and dysregulation of free cypD.

Similarly to the majority of previous *in vitro* studies investigating the interaction between mitochondrial biomolecules (including the study of interaction between cypD and Aβ[17] or interaction between 17β-HSD10 and Aβ[21]), we performed the binding experiments predominantly at a temperature of 25 °C. However, comparative experiments carried out under selected environmental conditions at an elevated temperature of 37 °C (temperature of living mitochondria) showed that the binding between 17β-HSD10 and cypD occurs at both the temperatures and that a change in the temperature of 12 °C does not have substantial effect on the interaction.

In the second part of study, we have shown that Aβ affects the binding between 17β-HSD10 and cypD and that the two different fragments of Aβ ($Aβ_{1–40}$ and $Aβ_{1–42}$) influence the binding in a different manner (Fig. 8). Whereas $Aβ_{1–42}$ facilitates the binding between 17β-HSD10 and cypD, $Aβ_{1–40}$ seems to suppress it. We believe that this difference can be explained by the different ability of $Aβ_{1–40}$ and $Aβ_{1–42}$ to form oligomers (oligomerization of $Aβ_{1–42}$ proceeds much faster than that of $Aβ_{1–40}$)[8,9]. The oligomers bind to 17β-HSD10 and the resulting complexes further bind to the immobilized cypD forming a tri-complex, whereas the monomeric Aβ is not able to bind to the two proteins simultaneously. However, with progressing oligomerization of Aβ, its ability to bind cypD decreases (Fig. 10). Interestingly, the ability to bind cypD decreases with the same time constant for $Aβ_{1–42}$ as for 17β-HSD10/$Aβ_{1–42}$. This suggests that the degree of oligomerization of $Aβ_{1–42}$ affects both the binding events (binding of individual $Aβ_{1–42}$ and binding of 17β-HSD10/$Aβ_{1–42}$) in the same fashion. This may be explained by the assumption that both these binding events are driven by the same interaction. Therefore, we hypothesize that the binding of 17β-HSD10/$Aβ_{1–42}$ complex to cypD takes place through $Aβ_{1–42}$.

Our results support the hypothesis by Stern and Yan[14] who postulated that the presence of Aβ affects the ability of 17β-HSD10 to regulate cypD. However, in contrast to Stern and Yan who suggested that the 17β-HSD10/cypD complex may dissociate in the presence of Aβ, we show that a tri-complex consisting of 17β-HSD10, cypD and $Aβ_{1–42}$ is formed. We suggest that each Aβ form participates in the dysregulation of cypD differently. At physiological concentrations, $Aβ_{1–40}$ remains monomeric and binds 17β-HSD10, thus inhibiting its regulation of free cypD. During AD, Aβ (both fragments $Aβ_{1–40}$ and $Aβ_{1–42}$) accumulates in the mitochondrial matrix, resulting in an increased binding of $Aβ_{1–40}$ to 17β-HSD10 and consequently in an increased level of free cypD triggering the apoptotic processes. $Aβ_{1–42}$ forms a tri-complex with both proteins, thus preventing cypD from translocating to the inner membrane. Excessive oligomerization of $Aβ_{1–42}$ related to AD, suppresses the ability of the 17β-HSD10/$Aβ_{1–42}$ complex to bind cypD, which leads to upregulation of cypD and apoptosis (similarly to $Aβ_{1–40}$). However, it should be noted that at high concentrations $Aβ_{1–40}$ also form oligomers[8,9] and thus we expect that with progressing AD, the properties of $Aβ_{1–40}$ may approach those of $Aβ_{1–42}$.

Conclusions

In this study, we show, for the first time, that two proteins related to pathogenesis of Alzheimer's disease, 17β-HSD10 and cypD, interact and form a stable complex. The study was performed *in vitro* using the SPR biosensor method; however, we set the experimental conditions in such a way that their key relevant characteristics approached those in the mitochondrial matrix. We have also shown that the interaction between 17β-HSD10 and cypD is sensitive to the ionic composition of the environment. This suggest that changes in the ionic composition which take place in the mitochondrial matrix can impair the regulation of cypD by 17β-HSD10 and lead to apoptosis. In addition, we have demonstrated that the presence of Aβ affects the binding between 17β-HSD10 and cypD and that different fagments of Aβ influence the binding through different mechanisms. While monomeric Aβ can only bind the two proteins separately, oligomeric Aβ can form a tri-complex with 17β-HSD10 and cypD. Increased concentrations and the degree of oligomerization of Aβ during Alzheimer's disease may hamper the interaction between 17β-HSD10 and cypD, which may result in the dysregulation of cypD by 17β-HSD10 and apoptosis *via* increased opening of mitochondrial permeability transition pores.

Methods

Reagents. NaCl, NaOH, KCl, $MgCl_2$, $CaCl_2$, bovine serum albumin (BSA) and all buffers: sodium acetate (SA10; 10 mM, pH 5.0), MES (10 mM, pH 5.0), HEPES (10 mM), high ionic strength phosphate-buffered saline (PBS_{Na}; 10 mM phosphate, 2.9 mM KCl, 750 mM NaCl, pH 7.4), were purchased from Sigma-Aldrich, Czech Republic. Oligoethylene glycol thiols 11-mercapto-hexa(ethyleneglycol)undecyloxy acetic acid (HS-C_{11}-$(EG)_6$-OCH_2-COOH) and 11-Mercapto-tetra(ethyleneglycol)undecanol (HS-C_{11}-$(EG)_4$-OH) were purchased from Prochimia, Poland. Ethanolamine hydrochloride (EA), 1-ethyl-3-(3-dimethylaminopropyl)-carbodiimide hydrochloride (EDC) and *N*-hydroxysuccinimide (NHS) were purchased from Biacore, Sweden. All buffers were prepared using deionized Milli-Q water (Merck, Czech Republic). 17β-HSD10 (human, recombinant), cypD (human, recombinant) and an antibody against cypD (Ab(cypD)) were purchased from Fitzgerald, USA, and an antibody against 17β-HSD10 (Ab(17β-HSD10)) from Biolegend, USA. $Aβ_{1–40}$ and $Aβ_{1–42}$ (human, synthetic) were obtained from AnaSpec, USA.

Surface plasmon resonance (SPR) biosensor. We used a six-channel laboratory SPR biosensor platform based on the prism coupling and wavelength spectroscopy of surface plasmons (Plasmon VI) interfaced with a dispersionless microfluidic system, both developed at the Institute of Photonics and Electronics, Prague[40]. In this platform, the angle of incidence of the light beam is fixed and changes in the excitation (resonance) wavelength of surface plasmons are measured by analysing the spectrum of polychromatic light reflected from an SPR chip attached to the prism coupler. The resonance wavelength is sensitive to changes in the refractive index caused by the binding of molecules to the surface of an SPR chip. In the used platform (resonance wavelength of 750 nm), a shift of 1 nm in the SPR wavelength represents a change in the protein surface coverage of 17 ng/cm^2. The SPR chips used in this study were prepared by coating microscope glass slides (Marienfeld, Germany) with thin layers of titanium (1–2 nm) and gold (48 nm) prepared via e-beam evaporation in vacuum. The SPR platform was equipped with a temperature stabilization module capable of maintaining a temperature within the microfluidic flow cell with a precision of 0.01 °C. All experiments were performed at a temperature of 25 °C and a flow rate of 20 µl/min unless explicitly stated otherwise.

Prior to the experiments, the surface of an SPR chip was modified by a self-assembled monolayer of mixed thiols, on which Ab(cypD) was immobilized using the amino-coupling method as described previously[41]. Briefly, a clean SPR chip was immersed in a 3:7 molar mixture of HS-C_{11}-$(EG)_6$-OCH_2-COOH and HS-C_{11}-$(EG)_4$-OH (ethanol solution, total concentration of 0.2 mM), then incubated for 10 minutes at 40 °C and then for at least 12 h at room temperature in the dark. Prior to use, the chip was rinsed with ethanol, Milli-Q water, dried with a stream of nitrogen and immediately mounted into the SPR biosensor. First, the mixture of 12.5 mM NHS and 62.5 mM EDC (in Milli-Q water) was injected (10 minutes) to activate carboxylic groups. Then, Ab(cypD) at concentration of 10 µg/ml in SA10 was pumped through the flow cell until the response to the immobilized Ab(cypD) levelled off (~12 minutes). Then PBS_{Na} was applied (5 minutes) to remove the non-covalently attached Ab(cypD) from the surface. Finally, 500 mM EA was injected (5 minutes) to deactivate the unreacted carboxylic groups. The SA10 running buffer was exchanged for MES and then detection channels were exposed to 90 nM cypD in MES to reach surface saturation (~15 minutes), while the reference channels were kept in MES. Then, all the channels were switched to MES for at least 20 minutes and PBS_{Na} was applied (5 minutes) to remove the non-specifically bound cypD molecules (see Supplementary Fig. S1a for a typical example of the sensorgram for the immobilization of cypD). SPR chips used in the experiments in which 17β-HSD10, cypD and Aβ were incubated in solution, were treated in the same manner, except for the following differences. After the immobilization of Ab(cypD), PBS_{Na} was injected (1 minute) and 10 µg/ml BSA was pumped through the flow cell until the sensor response of 1.5 nm was reached. Subsequently, PBS_{Na} was injected (5 minutes) followed by 500 mM EA (5 minutes) (see Supplementary Fig. S1b for a typical example of the sensorgram for the immobilization of Ab(cypD)).

Experimental: Study of interaction between 17β-HSD10 and cypD under variable environmental conditions. In this part of our study, cypD was immobilized on the surface of an SPR chip and the binding of 17β-HSD10 dissolved in different running buffers (containing different levels of ions or having different pH) was investigated. We used running buffers with: 1) varying concentrations of K^+, Mg^{2+} and Ca^{2+} to study the effect of individual ions at pH of 7.4 and 7.8, and 2) constant concentration of one ion (K^+ or Mg^{2+}) and varying concentration of the other to study the effect of combined ions at pH of 7.4.

For all the experiments in this study, the running buffer was flowed along the functionalized SPR chip until the stable sensor baseline was reached. A solution of 500 nM 17β-HSD10 in the running buffer (V = 100 µl) was kept at 37 °C for 10 minutes after being freshly prepared to ensure a comparable degree of tetramerization of 17β-HSD10 in all the used samples. Then, the solution of 17β-HSD10 was diluted to 1:4 with the running buffer to obtain the final concentration of 100 nM and the sample was injected in both the detection (surface with immobilized cypD) and reference (surface without immobilized cypD) channels. The binding of 17β-HSD10 was observed for 7 minutes and then the running buffer was injected again. The surface of the SPR chip was then regenerated (up to five times) by injecting PBS_{Na} for 5 minutes. The final sensor response was determined as a difference between the responses of the detection and reference channels 3 minutes after switching to the running buffer. Each experiment was repeated at least three times on at least two independent SPR chips.

In the study of the effect of individual ions on the interaction between 17β-HSD10 and cypD, we used a running buffer composed of $HEPES_1$ (10 mM; 200 µg/ml BSA, 5 mM Na^+, pH 7.4), which was mixed with a constant volume of aqueous solutions of KCl, $MgCl_2$ or $CaCl_2$ at concentrations that ensured the same dilution of HEPES for all the studied concentrations of ions. The pH was adjusted by NaOH; NaCl was added to yield a concentration of 5 mM Na^+. The concentration ranges used in our study were 0–140 mM for K^+ and 0–2.5 mM for Mg^{2+} and Ca^{2+}. A running buffer composed of $HEPES_2$ (10 mM, 200 µg/ml BSA, 5 mM Na^+, pH 7.8) mixed with particular concentrations of KCl and $MgCl_2$ was used to study the effect of individual K^+ and Mg^{2+} over the concentration ranges of 0–140 mM for K^+ and 0–2.5 mM for Mg^{2+} at pH of 7.8.

In the study of the effect of combined ions on the interaction between 17β-HSD10 and cypD, a running buffer composed of $HEPES_1$ was used to which a constant volume of the mixture of KCl and $MgCl_2$ was added and concentrations of the ions were selected to obtain 15 mM K^+ with 0–1 mM Mg^{2+}, and 0.25 mM Mg^{2+} with 0–30 mM K^+, respectively.

In addition, we compared the formation of 17β-HSD10/cypD complex at two different temperatures (25 °C and 37 °C) for three representative environmental conditions: 1) 15 mM K^+, 0.1 mM Mg^{2+}, 2) 15 mM K^+, 1 mM Mg^{2+}, and 3) 140 mM K^+, 0.1 mM Mg^{2+} (all in $HEPES_1$ running buffer). The temperature was adjusted to 37 °C by the temperature control unit of the SPR sensor prior to the injection of 17β-HSD10.

Experimental: Study of interaction between 17β-HSD10 and cypD in the presence of Aβ. In this part of our study, two experimental formats were employed: (1) cypD was immobilized on the surface of an SPR chip and the binding of 17β-HSD10, $Aβ_{1–40}$, $Aβ_{1–42}$ or their mixtures was studied, and (2) samples containing

cypD, 17β-HSD10, $A\beta_{1-40}$, $A\beta_{1-42}$ or their mixtures were incubated in solution, flowed over an SPR chip with immobilized Ab(cypD) and the binding of Ab(17β-HSD10) was measured to determine the amount of attached 17β-HSD10/cypD complex. The concentrations of the interacting molecules (cypD, 17β-HSD10, and Aβ) were chosen with respect to previously published *in vitro* studies[15,17,21].

The first experimental format was employed in three different studies in which we investigated how the binding between 17β-HSD10 and cypD is affected by: (1) presence of $A\beta_{1-40}$ and $A\beta_{1-42}$, (2) excess of $A\beta_{1-40}$, and (3) degree of oligomerization of $A\beta_{1-40}$ and $A\beta_{1-42}$. In all these studies, initially, $HEPES_{FINAL}$ (10 mM HEPES, 200 μg/ml BSA, 5 mM Na^+, 15 mM K^+, 0.1 mM Mg^{2+}, pH 7.4) was pumped across an SPR chip functionalized with cypD until the stable baseline was obtained. Then, the sample was injected into both the detection (surface with immobilized cypD) and the reference (surface without immobilized cypD) channels. The binding of 17β-HSD10 was monitored for 7 minutes (in the study of the effects of $A\beta_{1-40}$ and $A\beta_{1-42}$) or for 10 minutes (in the study of the effects of the excess of $A\beta_{1-40}$ and degree of oligomerization of Aβ) and then $HEPES_{FINAL}$ was injected again. The final (reference-compensated) sensor response was determined as the difference between the sensor responses obtained in the detection and reference channels 10 minutes after switching to the running buffer.

In the first study we investigated the effect of two different fragments of Aβ ($A\beta_{1-40}$, $A\beta_{1-42}$) on the interaction between 17β-HSD10 and cypD. Solutions of 17β-HSD10, $A\beta_{1-40}$, $A\beta_{1-42}$ and mixtures of these (see Supplementary Table S1 for details on the solutions used) were prepared in $HEPES_{FINAL}$ (V = 100 μl) and incubated for 1 hour at 37 °C. After incubation, the solutions were diluted to 1:7.5 by $HEPES_{FINAL}$ to obtain a final concentration of 100 nM of 17β-HSD10, 500 nM of $A\beta_{1-40}$ and 500 nM of $A\beta_{1-42}$, respectively. To evaluate the effect of excess of Aβ, different concentrations of Aβ ($A\beta_{1-40}$ or $A\beta_{1-42}$) were investigated, while the final concentration of 17β-HSD10 was held constant at 100 nM. A set of solutions of $A\beta_{1-40}$ or $A\beta_{1-42}$ at concentrations of 0.375, 0.75, 1.5, 3.75, 7.5 μM and a set of solutions of $A\beta_{1-40}$ or $A\beta_{1-42}$ at concentrations of 0.375, 0.5625 (for $A\beta_{1-42}$ only), 0.75, 1.5, 3.75, 7.5 μM with 750 nM 17β-HSD10 in $HEPES_{FINAL}$ (V = 100 μl) were prepared and incubated for 1 hour at 37 °C. After the incubation, the solution was further diluted by $HEPES_{FINAL}$ to obtain final concentrations of 50, 75 (for $A\beta_{1-42}$ only), 100, 200, 500 and 1000 nM of Aβ and 100 nM 17β-HSD10. Subsequently, to study the effect of oligomerization, binding experiments were performed for different oligomerization times for Aβ ($A\beta_{1-40}$, $A\beta_{1-42}$). A solution of $A\beta_{1-40}$ (3.75 μM) and $A\beta_{1-42}$ (3.75 μM) in $HEPES_{FINAL}$ (V = 100 μl) was prepared and incubated for 0, 10, 30, 60 and 180 minutes at 37 °C. After the incubation, either 17β-HSD10 (15 μl, 0.5 mg/ml) or $HEPES_{FINAL}$ (15 μl) was added to the solution of $A\beta_{1-42}$ and $HEPES_{FINAL}$ (15 μl) was added to the solution of $A\beta_{1-40}$, and the solution was incubated for 10 more minutes. Then, the solution was diluted to 1:7.5 by $HEPES_{FINAL}$ to obtain final concentrations of 100 nM and 500 nM, for 17β-HSD10 and Aβ, respectively. A freshly prepared 100 nM $A\beta_{1-40}$ and 100 nM $A\beta_{1-42}$ were included in the experiment for comparison.

In the second experimental format, we incubated 17β-HSD10, cypD, and Aβ ($A\beta_{1-40}$ or $A\beta_{1-42}$) together at a molar ratio of 1:5:10. This ratio was chosen so that the majority of cypD captured by Ab(cypD) is present in the form of a complex. The solutions of 17β-HSD10, cypD, $A\beta_{1-40}$, $A\beta_{1-42}$ and different mixtures of these (see Supplementary Table S2 for details on the solutions used) were prepared in $HEPES_{FINAL}$ (V = 100 μl) and incubated for 3 hours at 37 °C. After the incubation, the samples were diluted to 1:7.5 by $HEPES_{FINAL}$ to obtain the final concentrations of 250 nM, 50 nM and 500 nM for 17β-HSD10, cypD, and Aβ, respectively, and then flowed along the surface of an SPR chip with the immobilized Ab(cypD). After a 20-minute period during which the binding occurred, the sample was replaced with the running buffer. Finally, the 17β-HSD10/cypD complex was identified by measuring the response of the sensor to the injection of Ab(17β-HSD10) at a concentration of 10 μg/ml for 10 minutes.

Data availability

The data that support the findings of the current study are available from the corresponding author upon reasonable request.

Received: 3 September 2019; Accepted: 29 October 2019;
Published online: 13 November 2019

References

1. Helmerhorst, E., Chandler, D. J., Nussio, M. & Mamotte, C. D. Real-time and Label-free Bio-sensing of Molecular Interactions by Surface Plasmon Resonance: A Laboratory Medicine Perspective. *Clin Biochem Rev* **33**, 161–173 (2012).
2. Ditto, N. T. & Brooks, B. D. The emerging role of biosensor-based epitope binning and mapping in antibody-based drug discovery. *Expert Opinion on Drug Discovery* **11**, 925–937 (2016).
3. Yasmeen, A. *et al*. Differential binding of neutralizing and non-neutralizing antibodies to native-like soluble HIV-1 Env trimers, uncleaved Env proteins, and monomeric subunits. *Retrovirology* **11** (2014).
4. Murphy, M. P. & LeVine, H. III Alzheimer's disease and the amyloid-beta peptide. *Journal of Alzheimer's disease: JAD* **19**, 311–323, https://doi.org/10.3233/JAD-2010-1221 (2010).
5. Gabelle, A. *et al*. Correlations between soluble α/β forms of amyloid precursor protein and Aβ38, 40, and 42 in human cerebrospinal fluid. *Brain Research* **1357**, 175–183, https://doi.org/10.1016/j.brainres.2010.08.022 (2010).
6. Suzuki, N. *et al*. An increased percentage of long amyloid beta protein secreted by familial amyloid beta protein precursor (beta APP717) mutants. *Science* **264**, 1336–1340, https://doi.org/10.1126/science.8191290 (1994).
7. Crouch, P. J. *et al*. Mechanisms of Aβ mediated neurodegeneration in Alzheimer's disease. *The International Journal of Biochemistry & Cell Biology* **40**, 181–198, https://doi.org/10.1016/j.biocel.2007.07.013 (2008).
8. Lührs, T. *et al*. 3D structure of Alzheimer's amyloid-β(1–42) fibrils. *Proceedings of the National Academy of Sciences of the United States of America* **102**, 17342–17347, https://doi.org/10.1073/pnas.0506723102 (2005).
9. Garai, K. & Frieden, C. Quantitative analysis of the time course of Aβ oligomerization and subsequent growth steps using tetramethylrhodamine-labeled Aβ. *Proceedings of the National Academy of Sciences of the United States of America* **110**, 3321–3326, https://doi.org/10.1073/pnas.1222478110 (2013).
10. Muirhead, K. E., Borger, E., Aitken, L., Conway, S. J. & Gunn-Moore, F. J. The consequences of mitochondrial amyloid beta-peptide in Alzheimer's disease. *The Biochemical journal* **426**, 255–270, https://doi.org/10.1042/bj20091941 (2010).

11. Benek, O. *et al*. A Direct Interaction Between Mitochondrial Proteins and Amyloid-beta Peptide and its Significance for the Progression and Treatment of Alzheimer's Disease. *Current medicinal chemistry* **22**, 1056–1085 (2015).
12. Manczak, M. *et al*. Mitochondria are a direct site of A beta accumulation in Alzheimer's disease neurons: implications for free radical generation and oxidative damage in disease progression. *Human molecular genetics* **15**, 1437–1449, https://doi.org/10.1093/hmg/ddl066 (2006).
13. Hansson Petersen, C. A. *et al*. The amyloid beta-peptide is imported into mitochondria via the TOM import machinery and localized to mitochondrial cristae. *Proc Natl Acad Sci USA* **105**, 13145–13150, https://doi.org/10.1073/pnas.0806192105 (2008).
14. Yan, S. D. & Stern, D. M. Mitochondrial dysfunction and Alzheimer's disease: role of amyloid-β peptide alcohol dehydrogenase (ABAD). *International Journal of Experimental Pathology* **86**, 161–171, https://doi.org/10.1111/j.0959-9673.2005.00427.x (2005).
15. Yan, Y. *et al*. Surface Plasmon Resonance and Nuclear Magnetic Resonance Studies of ABAD−Aβ Interaction. *Biochemistry* **46**, 1724–1731, https://doi.org/10.1021/bi061314n (2007).
16. Marques, A. T., Fernandes, P. A. & Ramos, M. J. Molecular dynamics simulations of the amyloid-beta binding alcohol dehydrogenase (ABAD) enzyme. *Bioorganic & Medicinal Chemistry* **16**, 9511–9518, https://doi.org/10.1016/j.bmc.2008.09.043 (2008).
17. Du, H. *et al*. Cyclophilin D deficiency attenuates mitochondrial and neuronal perturbation and ameliorates learning and memory in Alzheimer's disease. *Nature medicine* **14**, 1097–1105, https://doi.org/10.1038/nm.1868 (2008).
18. Du, H., Guo, L., Zhang, W., Rydzewska, M. & Yan, S. Cyclophilin D deficiency improves mitochondrial function and learning/memory in aging Alzheimer disease mouse model. *Neurobiology of Aging* **32**, 398–406, https://doi.org/10.1016/j.neurobiolaging.2009.03.003 (2011).
19. Yang, S.-Y., He, X.-Y. & Miller, D. Hydroxysteroid (17β) dehydrogenase X in human health and disease. *Molecular and Cellular Endocrinology* **343**, 1–6, https://doi.org/10.1016/j.mce.2011.06.011 (2011).
20. Rauschenberger, K. *et al*. A non-enzymatic function of 17beta-hydroxysteroid dehydrogenase type 10 is required for mitochondrial integrity and cell survival. *EMBO Mol Med* **2**, 51–62, https://doi.org/10.1002/emmm.200900055 (2010).
21. Lustbader, J. W. *et al*. ABAD directly links Abeta to mitochondrial toxicity in Alzheimer's disease. *Science* **304**, 448–452, https://doi.org/10.1126/science.1091230 (2004).
22. Rao, V. K., Carlson, E. A. & Yan, S. S. Mitochondrial permeability transition pore is a potential drug target for neurodegeneration. *Biochimica et Biophysica Acta (BBA) - Molecular Basis of Disease* **1842**, 1267–1272, https://doi.org/10.1016/j.bbadis.2013.09.003 (2014).
23. Du, H., Guo, L. & Yan, S. S. Synaptic Mitochondrial Pathology in Alzheimer's Disease. *Antioxidants & Redox Signaling* **16**, 1467–1475, https://doi.org/10.1089/ars.2011.4277 (2012).
24. Singh, P., Suman, S., Chandna, S. & Das, T. K. Possible role of amyloid-beta, adenine nucleotide translocase and cyclophilin-D interaction in mitochondrial dysfunction of Alzheimer's disease. *Bioinformation* **3**, 440–445 (2009).
25. Carlson, E. A. *et al*. Overexpression of 17β-hydroxysteroid dehydrogenase type 10 increases pheochromocytoma cell growth and resistance to cell death. *BMC cancer* **15**, 166 (2015).
26. Poburko, D., Santo-Domingo, J. & Demaurex, N. Dynamic regulation of the mitochondrial proton gradient during cytosolic calcium elevations. *The Journal of biological chemistry* **286**, 11672–11684, https://doi.org/10.1074/jbc.M110.159962 (2011).
27. Santo-Domingo, J. & Demaurex, N. The renaissance of mitochondrial pH. *The Journal of General Physiology* **139**, 415–423, https://doi.org/10.1085/jgp.201110767 (2012).
28. Ivannikov, M. V. & Macleod, G. T. Mitochondrial Free Ca^{2+} Levels and Their Effects on Energy Metabolism in Drosophila Motor Nerve Terminals. *Biophysical Journal* **104**, 2353–2361, https://doi.org/10.1016/j.bpj.2013.03.064 (2013).
29. Murphy, E. & Eisner, D. A. Regulation of intracellular and mitochondrial Na in health and disease. *Circulation research* **104**, 292–303, https://doi.org/10.1161/CIRCRESAHA.108.189050 (2009).
30. Augustynek, B. *et al*. What we don't know about mitochondrial potassium channels? *Postepy biochemii* **62**, 189–198 (2016).
31. Gout, E., Rebeille, F., Douce, R. & Bligny, R. Interplay of Mg^{2+}, ADP, and ATP in the cytosol and mitochondria: unravelling the role of Mg^{2+} in cell respiration. *Proc Natl Acad Sci USA* **111**, E4560–4567, https://doi.org/10.1073/pnas.1406251111 (2014).
32. Haumann, J. *et al*. Mitochondrial free [Ca^{2+}] increases during ATP/ADP antiport and ADP phosphorylation: exploration of mechanisms. *Biophys J* **99**, 997–1006, https://doi.org/10.1016/j.bpj.2010.04.069 (2010).
33. O'Rourke, B., Cortassa, S. & Aon, M. A. Mitochondrial Ion Channels: Gatekeepers of Life and Death. *Physiology (Bethesda, Md.)* **20**, 303–315, https://doi.org/10.1152/physiol.00020.2005 (2005).
34. Lee, J., Culyba, E. K., Powers, E. T. & Kelly, J. W. Amyloid-β forms fibrils by nucleated conformational conversion of oligomers. *Nature Chemical Biology* **7**, 602, https://doi.org/10.1038/nchembio.624, https://www.nature.com/articles/nchembio.624#supplementary-information (2011).
35. Garlid, K. D. & Paucek, P. Mitochondrial potassium transport: the K^+ cycle. *Biochimica et Biophysica Acta (BBA) - Bioenergetics* **1606**, 23–41, https://doi.org/10.1016/S0005-2728(03)00108-7 (2003).
36. Kaasik, A., Safiulina, D., Zharkovsky, A. & Veksler, V. Regulation of mitochondrial matrix volume. *American Journal of Physiology-Cell Physiology* **292**, C157–C163, https://doi.org/10.1152/ajpcell.00272.2006 (2007).
37. Zoeteweij, J. P., van de Water, B., de Bont, H. J. & Nagelkerke, J. F. Mitochondrial K^+ as modulator of Ca^{2+}-dependent cytotoxicity in hepatocytes. Novel application of the K^+-sensitive dye PBFI (K^+-binding benzofuran isophthalate) to assess free mitochondrial K^+ concentrations. *The Biochemical journal* **299**, 539–543 (1994).
38. Gout, E., Rébeillé, F., Douce, R. & Bligny, R. Interplay of Mg^{2+}, ADP, and ATP in the cytosol and mitochondria: Unravelling the role of Mg^{2+} in cell respiration. *Proceedings of the National Academy of Sciences of the United States of America* **111**, E4560–E4567, https://doi.org/10.1073/pnas.1406251111 (2014).
39. Jung, D. W., Apel, L. & Brierley, G. P. Matrix free magnesium changes with metabolic state in isolated heart mitochondria. *Biochemistry* **29**, 4121–4128, https://doi.org/10.1021/bi00469a015 (1990).
40. Špringer, T., Piliarik, M. & Homola, J. Surface plasmon resonance sensor with dispersionless microfluidics for direct detection of nucleic acids at the low femtomole level. *Sensor Actuat B-Chem* **145**, 588–591, https://doi.org/10.1016/j.snb.2009.11.018 (2010).
41. Špringer, T., Chadtová Song, X., Ermini, M. L., Lamačová, J. & Homola, J. Functional gold nanoparticles for optical affinity biosensing. *Analytical and Bioanalytical Chemistry* **409**, 4087–4097, https://doi.org/10.1007/s00216-017-0355-1 (2017).

Acknowledgements

The study was supported by AZV CR (16-27611A) project. The authors would like to acknowledge the contribution of Lucie Peštová, who contributed to the project by performing multiple SPR biosensing experiments.

Author contributions

E.H. and T. Š. designed and conducted the experiments. E.H., T.Š., Z.K. and J.H. participated in data analysis and interpretation of the results and contributed to the writing of the manuscript. Z.K. and J.H. were responsible for the research project. All authors read and approved the final manuscript.

Competing interests
The authors declare no competing interests.

Additional information
Supplementary information is available for this paper at https://doi.org/10.1038/s41598-019-53157-7.

Correspondence and requests for materials should be addressed to J.H.

Reprints and permissions information is available at www.nature.com/reprints.

Publisher's note Springer Nature remains neutral with regard to jurisdictional claims in published maps and institutional affiliations.